nature COMMUNICATIONS

OPEN

ARTICLE

Received 22 Jul 2010 | Accepted 11 Jan 2011 | Published 8 Feb 2011

DOI: 10.1038/ncomms1185

CSN-mediated deneddylation differentially modulates Ci^{155} proteolysis to promote Hedgehog signalling responses

June-Tai Wu[1,2], Wei-Hsiang Lin[3], Wei-Yu Chen[1], Yi-Chun Huang[4,5], Chiou-Yang Tang[3], Margaret S. Ho[3], Haiwei Pi[4] & Cheng-Ting Chien[1,3,5]

The Hedgehog (Hh) morphogen directs distinct cell responses according to its distinct signalling levels. Hh signalling stabilizes transcription factor cubitus interruptus (Ci) by prohibiting SCF^{Slimb}-dependent ubiquitylation and proteolysis of Ci. How graded Hh signalling confers differential SCF^{Slimb}-mediated Ci proteolysis in responding cells remains unclear. Here, we show that in COP9 signalosome (*CSN*) mutants, in which deneddylation of SCF^{Slimb} is inactivated, Ci is destabilized in low-to-intermediate Hh signalling cells. As a consequence, expression of the low-threshold Hh target gene *dpp* is disrupted, highlighting the critical role of CSN deneddylation on low-to-intermediate Hh signalling response. The status of Ci phosphorylation and the level of E1 ubiquitin-activating enzyme are tightly coupled to this CSN regulation. We propose that the affinity of substrate–E3 interaction, ligase activity and E1 activity are three major determinants for substrate ubiquitylation and thereby substrate degradation *in vivo*.

[1] Institute of Molecular Medicine, College of Medicine, National Taiwan University, Taipei 100, Taiwan. [2] Department of Medical Research, National Taiwan University Hospital, Taipei 100, Taiwan. [3] Institute of Molecular Biology, Academia Sinica, Taipei 115, Taiwan. [4] Department of Life Science, Chang-Gung University, Tao-Yuan 333, Taiwan. [5] Graduate Institute of Life Sciences, National Defense Medical Center, Taipei 114, Taiwan. Correspondence and requests for materials should be addressed to C.-T.C. (email: ctchien@gate.sinica.edu.tw).

In developing tissues, morphogens are produced and secreted from different sources to build concentration gradients that serve as positional information, directing cells of different distances away from the source to adapt distinct fates[1,2]. To pattern complex tissues with precision, it is conceivable that the intracellular signalling level should scale to the morphogen gradient[3–6]. The Hedgehog (Hh) family proteins are evolutionarily conserved. As secreted morphogens, they have been implicated in patterning the formation of vertebrate face, spinal cord and digits, and *Drosophila* eyes, wings and several others[4,7–10]. In *Drosophila* developing wing discs, Hh signalling involves at least three distinct mechanisms in regulating the zinc-finger transcription factor cubitus interruptus (Ci), namely, blocking the proteolysis of the transcriptional activator full-length Ci (Ci^{155}) (refs 11–13), enhancing Ci^{155} nuclear partitioning[14–17] and transactivation activity[18–20]. In the absence of Hh signalling, Ci^{155} is partially proteolysed to generate the transcriptional repressor Ci (Ci^{75}). Ci^{155} proteolysis requires consecutive phosphorylation of Ci^{155} by protein kinase A (PKA)[21,22], glycogen synthase kinase 3β (GSK3β)[23,24] and casein kinase I (CKI)[23,25], resulting in a high affinity for the F-box protein Slimb of the SCF^{Slimb} ubiquitin (Ub) ligase complex for ubiquitylation[13,26,27]. Although it had been demonstrated that Hh signalling stabilizes Ci^{155} by precluding phosphorylation-dependent ubiquitylation of Ci^{155} (refs 23,24), how graded Hh signals are translated into graded Ci^{155} proteolysis is not clear.

The Ub E3 ligase activities of SCF (skp1-cullin-*F*-box protein) and other types of cullin–RING ligases (CRLs) are regulated by the conjugation of the Ub-like polypeptide Nedd8 onto the cullin scaffold component of CRLs, a process known as neddylation[28,29]. Genetic analyses performed in neddylation pathway mutants of various species indicate that Nedd8 modification of cullins is essential for CRL activities[27,30–34]. For example, neddylation is required for SCF^{Slimb}-mediated Ci^{155} proteolysis in cells not receiving Hh, thus suppressing Hh-mediated gene activation[12]. Nedd8 conjugation at a conserved carboxy-terminal lysine in all cullin proteins facilitates the binding of the RING domain-containing protein Rbx1/ROC1 that recruits Ub-loaded E2s[29,35]. Furthermore, neddylation induces a conformational change of the Cul5 carboxy terminus, which facilitates the transfer of Ub onto substrates[36]. Consistently, neddylation reduces the K_m for E2 binding to CRL and increases the K_{cat} for substrate ubiquitylation, thus increasing the processivity of ubiquitylation[37]. It has been estimated that neddylation of SCF allows the processive addition of more than four Ubs in a productive substrate–SCF encounter[38]. The Nedd8 moiety on cullins can be deconjugated by the COP9 signalosome (CSN) complex, thus inactivating CRL ligase activities[39,40]. Similar to other reversible protein modifications, neddylation and deneddylation of cullins occur dynamically *in vivo*[30,41]. Little is known whether dynamic deneddylation of CRLs is indeed critical to the substrate stability through modulating the extent of substrate ubiquitylation *in vivo*.

To better understand the role of deneddylation in Ci^{155} stability, in response to the Hh gradient, in this study, we used the *Drosophila* wing disc as a model in which cells display distinct responses to the Hh morphogen because of their positions. We analysed the SCF^{Slimb}-mediated Ci^{155} proteolysis in mutants for *CSN*, *GSK3β* (*sgg* in *Drosophila*), *Cul1*, *slimb* and E1 Ub-activating enzyme *uba1*. Taken together, our results suggest that deneddylation by regulating SCF^{Slimb} activity protects a portion of partially phosphorylated Ci^{155} from proteolysis, thus establishing the low-threshold Hh signalling responses.

Results

CSN deneddylation regulates the protein stability of Slimb. Whereas neddylation of cullins promotes CRL activities, deneddylation of cullins also promotes substrate degradation, mainly through protecting cullins and substrate receptors from neddylation-induced degradation[42–46]. To test whether protection of substrate receptors by deneddylation is a general rule, we first examined the protein stability of Slimb, a substrate receptor for the SCF complex that ubiquitylates several substrates including Ci^{155} (refs 13,47). Mutant clones for the CSN catalytic subunit CSN5 ($CSN5^{null}$) were generated in third-instar wing discs that also carry the *myc-slimb* transgene under the control of the ubiquitous *tubulin* promoter. In $CSN5^{null}$ cells, the protein level of Myc-Slimb is diminished (arrow in Fig. 1a), suggesting that the CSN is required to stabilize Slimb *in vivo*. In contrast, neddylation promotes Myc-Slimb turnover, as Myc-Slimb accumulates to high levels in cells homozygous for $Nedd8^{AN015}$ (arrow in Fig. 1b). To test whether the SCF-Slimb interaction is essential for neddylation-mediated Slimb turnover, we examined the protein stability of Myc-SlimbΔfbx that cannot be incorporated into the SCF complex because of the truncation of the F-box[47]. In contrast to the full-length Slimb, the protein levels of SlimbΔfbx in $CSN5^{null}$ mutant and neighbouring wild-type cells are indistinguishable (Fig. 1c). Taken together, we conclude that the substrate receptor Slimb, when incorporated into the SCF complex, is regulated by neddylation-induced degradation. However, neddylation-induced degradation of substrate receptors is unlikely a general rule, as the protein level of the Flag-conjugated

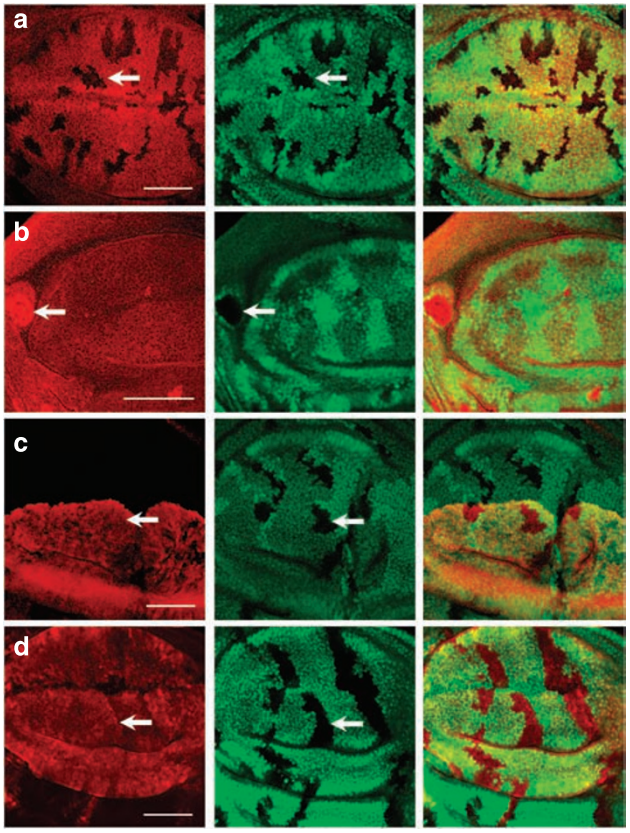

Figure 1 | Effects of neddylation and deneddylation on F-box proteins Slimb and Ago. (**a**) $CSN5^{null}$ clones generated in *Drosophila* third-instar larval wing discs are revealed by the absence of GFP (green). The protein level of *tubulin* promoter-driven *myc-slimb* (red) decreases in GFP-negative $CSN5^{null}$ clones (arrow). (**b**) $Nedd8^{AN015}$ clones marked by the absence of GFP (green) were generated in wing discs expressing Myc-Slimb. The level of Myc-Slimb (red) in $Nedd8^{AN015}$ clones is higher (arrow) compared with wild type. (**c**) The level of Myc-SlimbΔfbx (red) expressed by *ap-GAL4* is unaltered by $CSN5^{null}$ mutation (arrow) in the dorsal compartment of wing discs. (**d**) GFP-negative $CSN5^{null}$ clones are generated in wing discs (green), in which Flag-Ago (red) is expressed in wing pouches under the control of *ms1096-GAL4*. Flag-tag staining of Flag-Ago protein has a comparable signal level in wild-type and $CSN5^{null}$ cells (arrow). Scale bars, 50 μm.

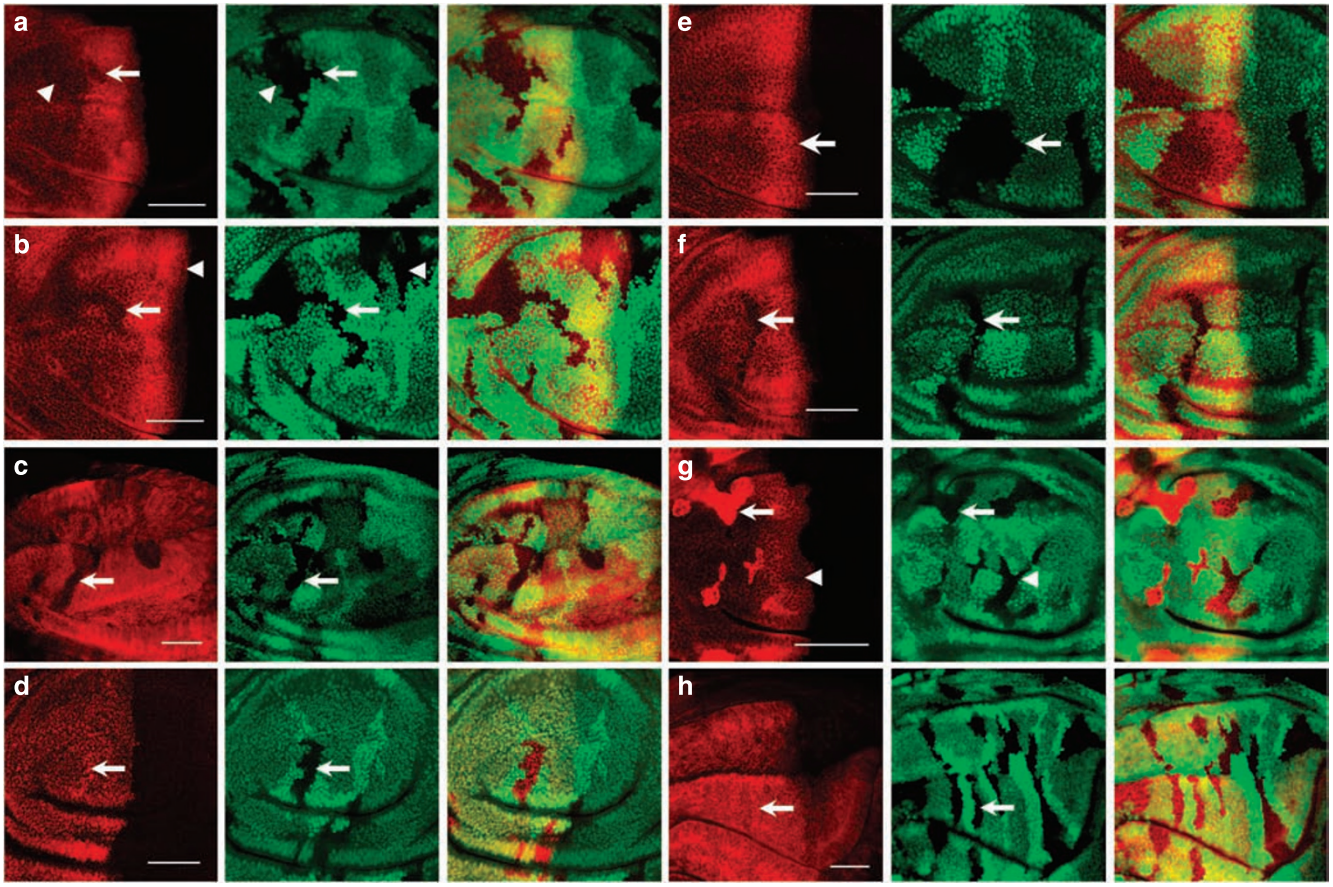

Figure 2 | The CSN positively regulates Ci^{155} protein stability in wing discs. (**a**) *CSN5^{null}* clones are revealed by the absence of GFP (green) in wing discs. Ci^{155} stained with the 2A1 antibody (red) is reduced in *CSN5^{null}* clones located in the A compartment, with arrow indicating mutant cells in the low-to-intermediate Hh signalling region and arrowhead indicating cells in the low Hh signalling region. (**b**) GFP-negative *CSN4^{null}* clones were generated in wing discs (green). Ci^{155} staining (red) is lower in the *CSN4^{null}* cells in the A compartment (arrow) than in the wild-type cells. The Ci^{155} levels in *CSN4^{null}* and wild-type cells located in A/P boundary are similar (arrowhead). (**c**) *CSN4^{null}* clones revealed by the absence of GFP (green) were generated in wing discs that simultaneously express *UAS-ci-myc* under the control of *ms1096-GAL4*. Protein levels of Ci-Myc detected by the anti-Myc antibody (red) are reduced in *CSN4^{null}* mutant clones (arrow). (**d**) The *ci-lacZ* expression (red) is not reduced in *CSN4^{null}* mutant clones (arrow) generated in wing discs. (**e**) GFP-negative *CSN5^{null}* clones (green) were generated in wing discs expressing wild-type *CSN5* construct under the control of *ms1096-GAL4*. Expression of wild-type CSN5 rescues the Ci^{155} level (red) in *CSN5^{null}* clones (arrow). (**f**) Expression of CSN5^{D148N}, which loses deneddylation activity, fails to rescues the Ci^{155} level (red) in *CSN5^{null}* clones (arrows). (**g**) *slimb^{P1493}*, *CSN5^{null}* clones revealed by the absence of GFP (green) in wing discs show Ci^{155} (red) accumulation in the A compartment (arrow) except when located adjacent to the A/P boundary (arrowhead). (**h**) The Ci-3P mutant protein (red), carrying mutations in three PKA phosphorylation sites, is ectopically expressed in *CSN4^{null}* mosaic wing pouches under the control of *ms1096-GAL4*. There is no difference in Ci-3P expression in wild-type and GFP-negative *CSN4^{null}* cells (arrow). Scale bars in all panels represent 50 μm.

F-box protein Archipelago (Flag-Ago) is unaltered in *CSN5^{null}* cells (Fig. 1d), suggesting that neddylation and deneddylation regulate the protein stability of some but not all of the SCF substrate receptors in *Drosophila*.

Reduction in the protein levels of Slimb and Cul1[42] in *CSN* mutants could promote the accumulation of SCF^{Slimb} substrates. This was tested by examining the protein level of a typical SCF^{Slimb} substrate Armadillo (Arm), the *Drosophila* ortholog of β-catenin[13,27]. In line with recent reports[48,49], the Arm level in *CSN5^{null}* cells is slightly but consistently higher than that in wild-type cells (Supplementary Fig. S1).

Deneddylation enhances Ci^{155} stability. We also tested how deneddylation regulates another SCF^{Slimb} substrate Ci^{155} in wing discs[13,27]. Unlike the increased level of Arm, the Ci^{155} protein level is instead downregulated in both *CSN5^{null}* and *CSN4^{null}* mutant cells (Fig. 2a,b), suggesting that neddylated SCF^{Slimb} degrades more Ci^{155}, despite the reduced levels of both Cul1[42] and the substrate receptor Slimb (Fig. 1a) in *CSN* mutants. Thus, Ci^{155} proteolysis is more sensitive to the level of neddylation, but less so to the bulk concentrations of SCF^{Slimb} components. In comparison to mutant clones in the low Hh signalling region (arrowhead in Fig. 2a), the reduction in the Ci^{155} level is more prominent in low-to-intermediate Hh signalling regions (arrow in Fig. 2a) in which the Ci^{155} protein level starts to fall but has not yet reached the basal level. Deneddylation upregulates the Ci^{155} level by a post-transcriptional mechanism, as we found that the protein levels of *ci-myc* and *HA-ci* transgenes under the *ms1096-GAL4* driver are reduced in *CSN* mutant cells (arrow in Fig. 2c and Supplementary Fig. S2). Furthermore, the expression of *ci-lacZ* that recapitulates *ci* transcription remains constant in *CSN5^{null}* cells (Fig. 2d).

It has been shown that IκBα is less stable in *CSN* mutants because of the inactivation of the CSN-associated deubiquitinase USP15, rather than a deneddylation-related mechanism[50]. In the case of Ci^{155} proteolysis, CSN-mediated deneddylation is indeed required for the regulation of Ci^{155} levels, as expression of wild-type *CSN5*, but not deneddylation-defective *CSN5^{D148N}*, restores the Ci^{155} level in *CSN5^{null}* clones (Fig. 2e,f). Downregulation of Ci^{155} in *CSN* mutant

cells is SCF^{Slimb} dependent, as Ci^{155} accumulates in *slimb^{P1493}CSN5^{null}* double-mutant cells (arrow in Fig. 2g). We noted that the Ci^{155} level remains unchanged in *slimb^{P1493}CSN5^{null}* double-mutant clones in the anterior/posterior (A/P) boundary region (arrowhead in Fig. 2g), in which Ci^{155} is subjected to Cul3- but not SCF-mediated proteolysis[27,51]. The Ci^{155} level in *CSN4^{null}* mutant clones that abuts the A/P boundary also remains unaltered (arrowhead in Fig. 2b), suggesting that the CSN regulates only SCF^{Slimb}-dependent Ci^{155} proteolysis. PKA phosphorylation of Ci^{155} is required for the interaction between Ci^{155} and Slimb[12,21,22], which should be important for the CSN to regulate SCF^{Slimb}-dependent Ci^{155} proteolysis. The HA-Ci-3P protein that contains three mutated PKA phosphorylation sites and resistant to SCF^{Slimb}-mediated proteolysis[22] appears to have comparable expression levels in *CSN4^{null}* mutant and wild-type cells (Fig. 2h). This is in contrast to the wild-type Ci-Myc and HA-Ci that are decreased in *CSN* mutant cells (Fig. 2c and Supplementary Fig. S2). Therefore, the CSN complex regulates the Ci^{155} levels through the SCF^{Slimb} machinery in the A compartment of wing discs, except at the A/P boundary region.

CSN differentially regulates Ci^{155} proteolysis. To gain insights into how the CSN regulates SCF^{Slimb}-mediated Ci^{155} proteolysis, the proportions of proteolysed and stable Ci^{155} along the A/P axis of wing discs were quantified. We generated random mosaic twin clones from double heterozygotes for the *Cul1^{EX}* and *CSN4^{null}* alleles, both located at chromosome 2R (Fig. 3a). One of the twin clones is homozygous for *Cul1^{EX}*, marked with the double-brightness of green fluorescent protein (GFP) signal, and the other twin clone is homozygous for *CSN4^{null}*, marked by the complete absence of GFP signal. Cells marked by single brightness of GFP signal are double heterozygous for *Cul1^{EX}* and *CSN4^{null}*, which are considered as wild-type control. The Ci^{155}-expressing A compartment of wing pouches was divided into 12 equal regions, with the most anterior cells being in region 1 and cells receiving the highest level of Hh in region 12 (Fig. 3b). We measured the Ci^{155} protein levels in *Cul1^{EX}*, *CSN4^{null}* and wild-type control cells in regions 1–12. The percentage of Ci^{155} that has undergone SCF^{Slimb}-dependent proteolysis in each region was calculated as the Ci^{155} level in *Cul1^{EX}* cells (no proteolysis) subtracted by the Ci^{155} level in double-heterozygous cells (normal proteolysis in wild-type control), which is then normalized to the Ci^{155} level in *Cul1^{EX}* cells: percentage of Ci^{155} proteolysis = $([Ci^{155}]^{Cul1EX} - [Ci^{155}]^{wild\text{-}type})/[Ci^{155}]^{Cul1EX}$. We found that the extent of SCF^{Slimb}-dependent Ci^{155} proteolysis is constantly high across regions 1–8, and gradually declines from region 8 to 12 (Fig. 3c). We also quantified the extents of SCF^{Slimb}-dependent Ci^{155} proteolysis in *CSN4^{null}* cells across regions 1–12 using the same methodology: percentage of Ci^{155} proteolysis = $([Ci^{155}]^{Cul1EX} - [Ci^{155}]^{CSN4null})/[Ci^{155}]^{Cul1EX}$. Interestingly, Ci^{155} proteolysis in *CSN4^{null}* cells remained similar to wild-type cells in regions 1–8, and graded Ci^{155} proteolysis in *CSN4^{null}* cells was also present from regions 8 to 12. Remarkably, Ci^{155} proteolysis is prominently enhanced in *CSN4^{null}* cells in regions 9, 10 and 11 compared with wild-type cells in the same regions, with 30, 40 and 24% reductions in the Ci^{155} levels, respectively (Fig. 3c). In region 12 closest to the A/P boundary in which the protein level of Ci^{155} is regulated by the Cul3-organized CRL[27,51], the proportion of SCF^{Slimb}-dependent Ci^{155} proteolysis is unaltered in *CSN4^{null}* mutant cells (arrow in Fig. 3a and arrowhead in Fig. 2b). Mild enhancements of 1–6% of Ci^{155} proteolysis were noted in *CSN4^{null}* cells in regions 1–8, although these differences were not statistically significant except for regions 6 and 7 ($n \geq 6$, $P < 0.05$ by Student's *t*-test). On the basis of the proteolytic curves of Ci^{155} in wild-type and *CSN4^{null}* cells, we propose that proteolysis-resistant Ci^{155} in wild-type cells is composed of 'stable' and 'conditionally stable' forms, the latter being stable in wild-type cells but proteolysed in *CSN* mutant cells by SCF^{Slimb}, whereas the former is insensitive to the absence of CSN activity. The levels of conditionally stable Ci^{155} are highest in regions 9–11, in which cells are exposed to low-to-intermediate levels of Hh.

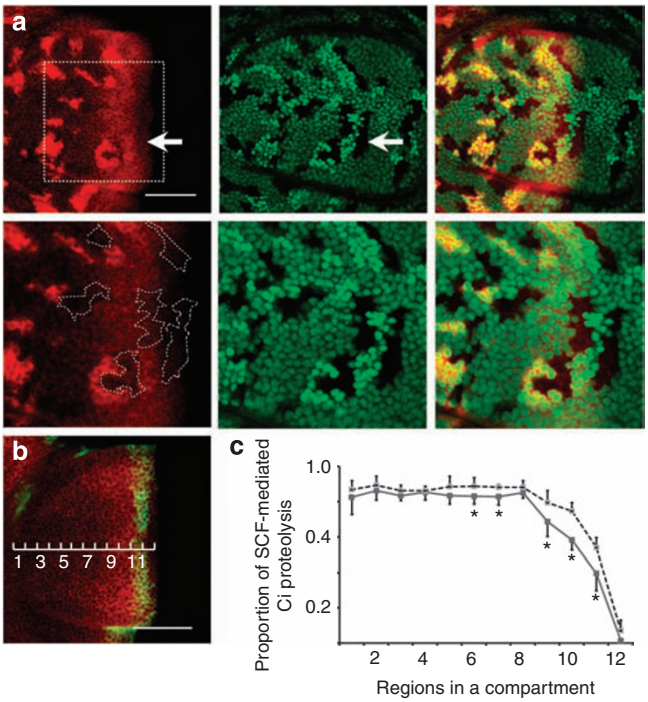

Figure 3 | The CSN regulates Ci^{155} proteolysis predominantly in intermediate Hh signalling regions. (**a**) Mutant clones for *CSN4^{null}* or *Cul1^{EX}* were generated simultaneously in the same wing discs of the *hsflp; FRT42D CSN4^{null}/FRT42D Cul1^{EX}, nlsGFP* genotype. Ci^{155} (red) levels stained by 2A1 antibody was measured in the following cells: *CSN4^{null}* mutant clones marked by the absence of GFP, *Cul1^{EX}* mutant clones marked by two copies of GFP and double-heterozygous *CSN4$^{null/+}$*, *Cul1$^{EX/+}$* cells marked by one copy of GFP (green). The lower panels in **a** show close-up images of a region near the A/P boundary (outlined by a dashed square in upper left panel), with some *CSN4^{null}* clones highlighted by white dashed lines (lower left panel). (**b**) The A compartment of wing pouches showing expression of Ci^{155} (red) and *dpp-lacZ* (green) is divided equally into 12 regions along the A/P axis. Expression of *dpp-lacZ* is detected in region 11. Scale bars represent 50 μm (**a**, **b**). (**c**) The portions of Ci^{155} that undergo SCF^{Slimb}-mediated proteolysis in regions 1–12 of wild-type (grey line) and *CSN4^{null}* mutant cells (dashed line) were calculated. Averaged Ci^{155} pixel intensities for each region ($n \geqq 6$) are shown. Asterisks indicate a significant difference of Ci^{155} proteolysis between wild-type and *CSN4^{null}* ($P < 0.05$). Error bars present the standard deviation.

CSN is required for Hh-dependent wing patterning. To examine whether the level of conditionally stable Ci^{155} is essential for distinct cell fates directed by graded Hh signalling, we assayed the activation of Hh-responsive, position-specific genes, such as *ptc* and *dpp*, whose expression represent high and low Hh signalling responses, respectively[19]. Interestingly, we found that the expression of *dpp-lacZ* is significantly repressed in *CSN4^{null}* mutant cells (arrow in Fig. 4a), whereas the Ptc protein level and the expression of *ptc-lacZ* remain unaltered (arrows in Fig. 4b,c), indicating a critical role of the conditionally stable Ci^{155} for the Hh-mediated *dpp* expression. The expression of *engrailed* (*en*) is regulated by high Hh signalling activity in the A/P boundary[52]. We tested whether *en* expression in the A/P boundary is downregulated in *CSN4^{null}* mutant because of Ci^{155} proteolysis. En protein level is instead enhanced not only at the A/P boundary but also in A and P compartments, in which *en* expression is independent from Hh signalling (Fig. 4d), suggesting that *en* expression is subjected to another layer of regulation by the CSN.

To further substantiate the notion that small perturbations of the Ci^{155} level can inactivate *dpp* expression, we tested whether

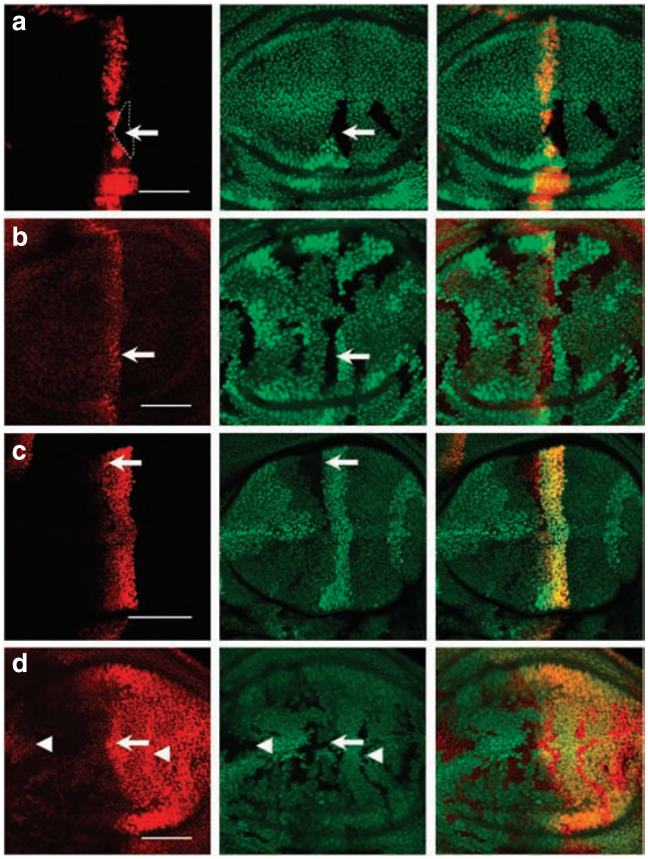

Figure 4 | The CSN differentially regulates Hh downstream gene expression. (**a**) A *CSN4*^{null} clone (indicated by the dashed outline) is generated in *dpp-lacZ* wing discs. *dpp-lacZ* expression detected by anti-β-gal antibody (red) is markedly repressed in *CSN4*^{null} cells (arrow). (**b**) *CSN5*^{null} clones indicated by the absence of GFP are generated in wing discs. Ptc (red) protein level in *CSN5*^{null} cells (arrow) detected by the monoclonal antibody Apa-1 is similar to that in wild-type cells. (**c**) *ptc-lacZ* staining (red) is comparable in wild-type and *CSN5*^{null} cells that are marked by the absence of GFP (arrow). (**d**) En protein levels (red) are increased in the *CSN5*^{null} cells (arrow) located in the A/P boundary as well as in the A and P compartments (arrowheads). Scale bars in all panels represent 50 μm.

ms1096-GAL4-driven *ci-RNAi*[53] could abolish *dpp-lacZ* expression. The *ms1096-GAL4* driver exhibits differential expression in wing pouches, with higher levels in the dorsal and lower levels in the ventral compartment. As a consequence, *dpp-lacZ* expression is detectable in the ventral compartment, but diminished in the dorsal compartment, in which the Ci^{155} level is comparably reduced as in *CSN5*^{null} cells (Supplementary Fig. S3). In contrast, the expression of *ptc-lacZ* remains unaltered in the dorsal compartment (Supplementary Fig. S3). Therefore, the *dpp-lacZ* expression is sensitive to small reductions in Ci^{155} levels. The expression of *dpp-lacZ* is downregulated by Ci[75], the transcriptional repressor produced by SCF^{Slimb}-mediated proteolysis of Ci^{155}, whereas Ptc expression is not[54]. Disruption of *dpp-lacZ* but not Ptc expression in *CSN* mutant cells suggests an alternative possibility that a higher level of Ci[75] accumulates in *CSN* mutant cells as a result of SCF^{Slimb}-mediated proteolysis.

Proper phosphorylation confers conditionally stable Ci^{155}. Our results suggest that low-to-intermediate Hh signalling (regions 9–11) renders the appearance of conditionally stable Ci^{155}, whereas high (region 12) and low (regions 1–8) Hh signalling activities do not. It has also been suggested that graded Hh signalling activities counteract Ci^{155} proteolysis by inhibiting different levels of Ci^{155} phosphorylation[55], leading to differential affinities to the F-box protein Slimb for SCF^{Slimb}-mediated proteolysis[26]. We therefore tested whether the phosphorylation status of Ci^{155} alters the level of conditionally stable Ci^{155}. Ci^{155} phosphorylation can be compromised by the ectopic expression of dominant-negative GSK3β (DN-GSK3β), resulting in the inhibition of Ci^{155} proteolysis in the low Hh signalling region[24]. Although proteolysed Ci^{155} in the low Hh region (regions 1–8) is 84±5% of total Ci^{155} in wild-type cells (Fig. 3c), it is reduced to 38±8% in the *DN-GSK3β* expression clones (averaged from seven clones in regions 1–8, arrowhead in Fig. 5a). Accumulation of Ci^{155} in regions 1–8, however, is suppressed by the *CSN4*^{null} mutation (arrow in Fig. 5a), with 75±11% of Ci^{155} undergoing proteolysis in *CSN4*^{null} mutant cells expressing *DN-GSK3β* ($n=8$). Thus, the accumulated Ci^{155} in regions 1–8 on *DN-GSK3β* wings is conditionally stable in nature, undergoing proteolysis in the absence of CSN activity. Likewise, inhibiting CKI kinase activity by expressing dominant-negative Doubletime (DN-DBT) causes Ci^{155} accumulation[25], which is also suppressed by the *CSN4*^{null} mutation, as shown by reduced Ci^{155} levels in *CSN4*^{null} mutant cells expressing *DN-DBT* (arrow, Fig. 5b) compared with wild-type cells expressing *DN-DBT*. Thus, lowering the phosphorylation level by inhibiting either GSK3β or CKI produces conditionally stable Ci^{155} in the low Hh signalling region, mimicking the Ci^{155} behaviour in the region with low-to-intermediate Hh signalling.

To examine the critical role of phosphorylation in the appearance of conditionally stable Ci^{155}, we examined whether the CSN regulates the protein levels of Ci mutants in which CKI or GSK3β phosphorylation sites are mutated (Ci-C1-3E and Ci-G2-3E, respectively). Both Ci-C1-3E and Ci-G2-3E cannot be proteolysed efficiently in the absence of Hh signalling[26]. When ectopically expressed in wing pouches by *ms1096-GAL4*, the protein levels of Ci-C1-3E or Ci-G2-3E are downregulated by the *CSN4*^{null} mutation (arrows in Fig. 5c,d), suggesting that Ci-C1-3E and Ci-G2-3E represent the CSN-regulated, conditionally stable forms of Ci.

Expression of the PKA regulatory subunit, PKA-R*, inhibits PKA-dependent Ci^{155} phosphorylation and precludes PKA-primed sites for further GSK3β and CKI phosphorylation[21]. We therefore examined the effect of further reducing Ci^{155} phosphorylation on the CSN-dependent Ci^{155} stabilization. Under the control of *C765-GAL4*, the PKA-R* expression enhances Ci^{155} levels across the A compartment. However, no downregulation of Ci^{155} levels could be detected in *CSN4*^{null} mutant cells expressing *PKA-R**, including those in intermediate-to-high and low Hh signalling regions (arrowhead and arrow in Fig. 5e, respectively). Therefore, phosphorylation-depleted Ci^{155} is unlikely to be the CSN-regulated conditionally stable form.

The above analysis also suggests that lack of PKA phosphorylation in the high Hh signalling region 12 may account for the absence of conditionally stable Ci^{155}. To test this, Ci^{155} phosphorylation by PKA is induced by expressing the catalytic subunit mC* under the control of *ms1096-GAL4*[23]. Expression of mC* equalizes Ci^{155} levels across the A compartment, mainly because of the downregulation of Ci^{155} levels in intermediate-to-high Hh signalling regions and the upregulation in high Hh signalling region 12. However, the Ci^{155} levels in mC*-expressing *CSN5*^{null} mutant clones were reduced in large clones covering region 12 (arrows in Fig. 5f), as compared with mC*-expressing wild-type cells (arrowhead in Fig. 5f), an indication of the appearance of conditionally stable Ci^{155} even in the presence of high Hh signalling. Given that conditionally stable Ci^{155} appears in the low Hh signalling region on GSK3β or CKI inhibition and in the high Hh signalling region by PKA activation, these results support the idea that partially phosphorylated Ci^{155} represents the conditionally stable form regulated by the CSN.

Dominant-negative SlimbΔfbx fails to induce CSN regulation. To further corroborate the SCF-dependent mechanism for CSN

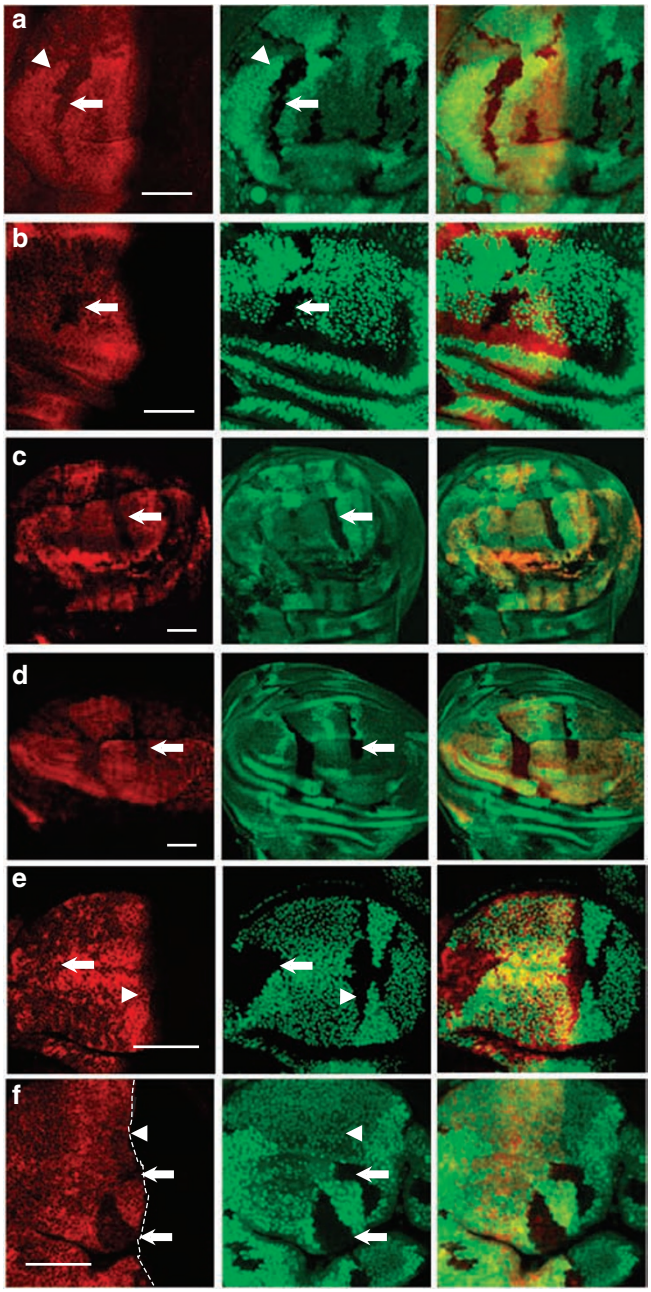

Figure 5 | Conditionally stable Ci^{155} is sensitive to phosphorylation levels. (**a**) *CSN4^{null}* clones are generated in wing discs that express dominant-negative GSK3β (DN-GSK3β) by *ms-1096-GAL4*. DN-GSK3β increases Ci^{155} expression (red) in low Hh signalling regions (arrowhead). The Ci^{155} level is downregulated in *CSN4^{null}* cells (arrow) in the presence of DN-GSK3β. (**b**) Inhibition of CKI activity by *C765-GAL4*-driven DN-DBT increases the accumulation of Ci^{155} (red) in wild-type cells. This accumulation of Ci^{155} is downregulated in *CSN4^{null}* clones (arrow). (**c**) *CSN4^{null}* clones marked by the absence of GFP (green) were generated in wing discs expressing *UAS-ci-C1-3E-myc* under the control of *ms1096-GAL4*. The Ci-C1-3E-Myc levels detected by anti-Myc antibody (red) were decreased in *CSN4^{null}* clones (arrow). (**d**) *CSN4^{null}* clones marked by the absence of GFP (green) were generated in wing discs expressing *UAS-ci-G2-3E-myc*. Ci-G2-3E-Myc (red) staining is decreased in *CSN4^{null}* clones (arrow). (**e**) Ectopic expression of PKA-R*, the regulatory subunit of PKA, by *C765-GAL4* increases Ci^{155} levels in the A compartment. The upregulated Ci^{155} levels (red) either in low or low-to-intermediate Hh regions (arrow and arrowhead, respectively) are not altered in *CSN5^{null}* clones in wing discs. (**f**) *CSN5^{null}* clones were generated in wing discs that express the catalytic subunit of PKA (PKA-mC*) by *ms-1096-GAL4*. Ci^{155} levels (red) near the A/P boundary in the high Hh signalling region is downregulated in *CSN5^{null}* clones (arrows) compared with wild-type cells (arrowhead). Dashed lines indicate the A/P boundary. Scale bars in all panels represent 50 μm.

regulation, we tested whether Ci^{155} has to be incorporated into the SCF complex for the CSN to confer its conditional stability. To do this, the F-box-truncated SlimbΔfbx protein that can competitively bind Ci^{155} but cannot be incorporated into SCF was ectopically expressed by *ap-GAL4* in wing discs. Higher levels of Ci^{155} detected in wing discs suggest that SlimbΔfbx-sequestered Ci^{155} is free from SCF-mediated proteolysis. Unlike the conditionally stable Ci^{155} upregulated by DN-GSK3β or DN-DBT expression, the upregulated Ci^{155} levels caused by SlimbΔfbx expression is insensitive to the absence of CSN activity in *CSN5^{null}* cells (arrow, Fig. 6a). Thus, Ci^{155} that binds the substrate receptor Slimb, but fails to form SCF^{Slimb}-Ci^{155} intermediates, is insufficient to produce conditionally stable Ci^{155}.

Although SlimbΔfbx-sequestered Ci^{155} is insensitive to the CSN regulation, the residual Ci^{155} protein that is free from SlimbΔfbx titration is still insensitive to the CSN regulation, arguing that the CSN regulation does not increase the concentration or availability of the SCF^{Slimb}-Ci^{155} intermediate. As the strong expression of SlimbΔfbx by *ap-GAL4* might sequester Ci^{155} from SCF regulation, *ms1096-GAL4* was used to express moderate levels of SlimbΔfbx in the dorsal compartment and low levels in the ventral compartment. Moderate depletion of the SCF^{Slimb}-Ci^{155} intermediates in the dorsal compartment by *ms1096-GAL4* behaved similarly to the strong depletion by *ap-GAL4*; no significant difference in Ci^{155} proteolysis was detected between wild-type and *CSN5^{null}* cells (arrowhead in Fig. 6b). Interestingly, although the Ci^{155} levels fluctuate in the ventral compartment because of weak depletion of the SCF^{Slimb}-Ci^{155} intermediates, they were still insensitive to any CSN modulation (arrow in Fig. 6b). In these experiments, the remaining Ci^{155} after SlimbΔfbx titration still possessed a high affinity for Slimb in low Hh signalling regions. Thus, in contrast to the perturbation by DN-GSK3β, different extents of perturbation on the concentration of tightly associated SCF^{Slimb}-Ci^{155} intermediates are invariantly insufficient to generate conditionally stable Ci^{155}.

Sensitivity of Ci^{155} proteolysis to the Ub supply. A compromised affinity between partially phosphorylated Ci^{155} and Slimb can result in reduced availability of SCF^{Slimb}-Ci^{155} intermediates. However, as shown in the SlimbΔfbx titration experiment, reduced availability of SCF^{Slimb}-Ci^{155} intermediates was insufficient to confer CSN regulation. We hypothesized that partial Ci^{155} phosphorylation may compromise the duration of SCF^{Slimb}-Ci^{155} association, disrupting substrate polyubiquitylation. In line with this idea, recent findings suggest that most of the encounters between SCF and its substrate are unproductive, with the dissociation rate k_{off} being much larger than the reaction rate of adding the first Ub (k_{ub1})[38]. Although most of the encounters between SCF and its substrate are unproductive, neddylation of SCF allows polyubiquitylation (k_{ub2-4}) to proceed at higher rates once the first Ub is added[38]. Therefore, CSN deneddylation could be critical at the Ub chain elongation step when the affinity between SCF and substrate is reduced, such as in the case of partially phosphorylated Ci^{155}. Processive Ci^{155} ubiquitylation would demand a constant supply of activated Ub, which could be sensitive to the level of the Ub-activating enzyme. In mosaic analysis with a repressible cell marker (MARCM) clones, in which *uba1-dsRNA* was expressed to knockdown the expression of the Ub-activating enzyme, accumulation of Ci^{155} (arrow in Fig. 6c) suggests that the insufficiency in supplying activated Ub leads to the disruption of Ci^{155} polyubiquitylation and proteolysis. The defect of

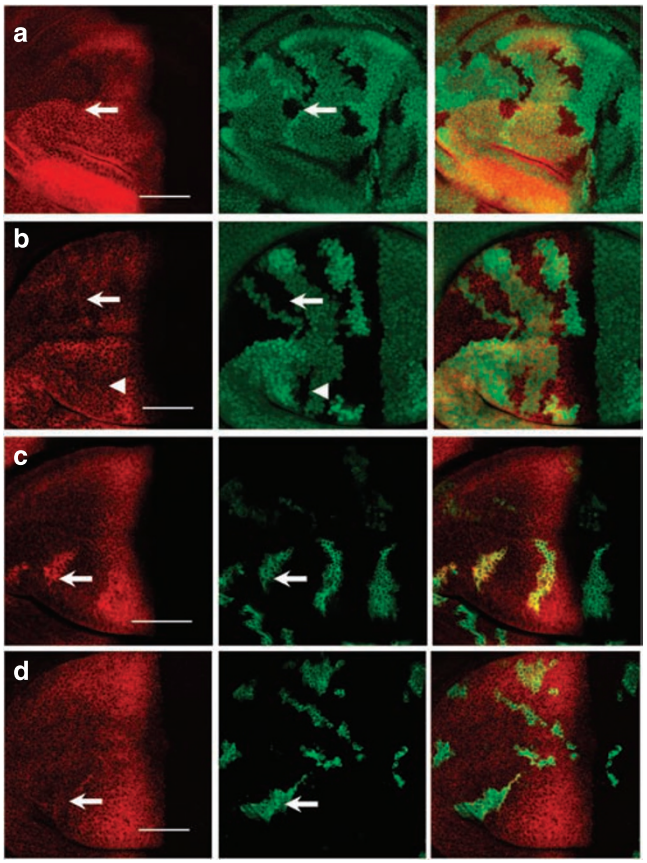

Figure 6 | CSN control of Ci^{155} levels upregulated by SlimbΔfbx or Uba1 depletion. (**a**) *CSN5^{null}* clones are generated in wing discs expressing Myc-SlimbΔfbx in the dorsal compartment under the control of *ap-GAL4*. Ectopic expression of SlimbΔfbx increases the levels of Ci^{155} (red) in the dorsal compartment. Moreover, the upregulated Ci^{155} is maintained in *CSN5^{null}* clones (arrow). (**b**) Under the control of *ms1096-GAL4,* the moderate level of ectopic Myc-SlimbΔfbx in the dorsal compartment causes similar accumulation of Ci^{155} (red) in both wild-type and *CSN5^{null}* cells (arrowhead); the lower level of ectopic Myc-SlimbΔfbx in the ventral compartment also causes similar accumulation of Ci^{155} in both wild-type and *CSN5^{null}* cells (arrow) (**c**) GFP-marked MARCM clones (green) expressing *uba1-dsRNA* by *ms1096-GAL4* generated in wing discs show upregulation of Ci^{155} (red) levels compared with adjacent wild-type cells that are negative for GFP. (**d**) GFP-marked *uba1-dsRNA* MARCM clones that are also *CSN5^{null}* show Ci^{155} levels (red) comparable with adjacent GFP-negative wild-type cells. Scale bars in all panels represent 50 μm.

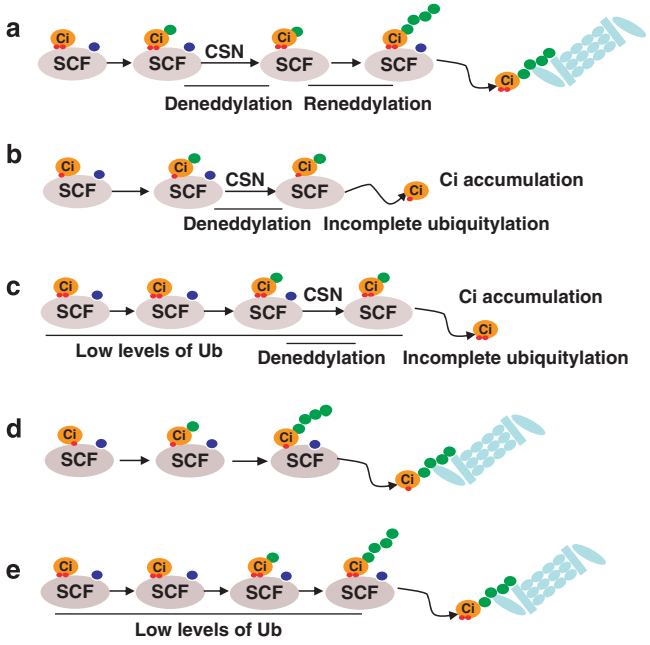

Figure 7 | Models for SCF^{Slimb}-mediated Ci^{155} proteolysis. Successful substrate polyubiquitylation requires collaboration of three components: adequate substrate–enzyme interaction time, persistent neddylated E3 ligase activity and high levels of activated ubiquitin supply. Green dot, ubiquitin; blue dot, Nedd8; and red dot, phosphate group. (**a**) For fully phosphorylated Ci^{155} that binds strongly to SCF in no-to-low Hh signalling regions, long substrate–enzyme binding duration allows complete polyubiquitylation, despite temporary inactivation of SCF ligase by CSN-mediated deneddylation. (**b**) In low-to-intermediate Hh signalling regions as well as in the presence of DN-GSK3β, partially phosphorylated Ci^{155} associates with SCF weakly. Dissociation of Ci^{155} from the SCF^{Slimb} complex following CSN-mediated deneddylation of SCF disrupts processive ubiquitylation of Ci^{155}. (**c**) Limited supply of activated ubiquitin could disrupt processive ubiquitylation of fully phosphorylated Ci^{155} in no-to-low Hh regions in the presence of CSN deneddylation. (**d**) *CSN* mutations allow the processivity of polyubiquitylation mediated by constantly neddylated SCF, which compensates for the short duration of interaction between SCF^{Slimb} and Ci^{155} in low-to-intermediate Hh signalling regions or in the presence of DN-GSK3β. (**e**) In no-to-low Hh regions, limited supply of activated ubiquitin in *uba1-dsRNA* cells interrupts Ci^{155} polyubiquitylation, which is suppressed by constitutively neddylated SCF in *CSN* mutants.

Ci^{155} accumulation in *uba1-dsRNA* cells is likely caused by reduced ubiquitylation, which could be compensated by constitutively neddylated SCF that promotes processivity of ubiquitylation. Indeed, the elevated Ci^{155} level in *uba1-dsRNA* knockdown cells was almost completely suppressed by introducing the *CSN5^{null}* mutation in the *uba1-dsRNA* MARCM clones (arrow in Fig. 6d). This result is consistent with the idea that inactivating the deneddylation machinery could compensate for inefficient polyubiquitylation in *uba1-dsRNA* knockdown cells, thereby restoring the assembly of proteasome-targeting polyubiquitin chains on Ci^{155}.

Discussion

In this study, we show that CSN-mediated deneddylation of SCF^{Slimb} is critical for the Ci^{155} stability in low-to-intermediate Hh regions in which partially phosphorylated Ci^{155} has a reduced affinity for the ubiquitylation machinery SCF^{Slimb}. The effect of CSN deneddylation on SCF^{Slimb} likely reduces ubiquitylation processivity, thus preserving 'conditionally stable Ci^{155}' in these low-to-intermediate Hh regions. We propose a broader view for CRL substrate degradation *in vivo*, determined by three interdependent factors: substrate-enzyme affinity, deneddylation-regulated CRL activity and the supply of Uba1-activated Ub. We propose that steady-state Ci^{155} levels are low in the low Hh signalling regions because processive polyubiquitylation of the tightly associated SCF^{Slimb}-Ci^{155} complex proceeds even with intermittent SCF^{Slimb} inactivation by CSN-mediated deneddylation (Fig. 7a). In low-to-intermediate Hh regions, the steady-state Ci^{155} levels are sensitive to CSN-mediated deneddylation as a result of weakened SCF^{Slimb}-Ci^{155} association, as in *DN-GSK3β* cells (Fig. 7b). In *uba1-dsRNA* cells, the Ci^{155} levels are sensitive to CSN-mediated deneddylation because of insufficient activated Ub (Fig. 7c). In these cases, we envision that processive polyubiquitylation becomes more difficult because of constant neddylation–deneddylation cycling by the CSN, and can be aborted by the dissociation of Ci^{155} from weakly associated SCF^{Slimb}-Ci^{155} or the lack of activated Ub. However, an insufficiency in Ci^{155} downregulation can be offset by constitutive neddylated SCF^{Slimb} in *CSN* mutants, which ubiquitylates substrates

processively on a single SCF^{Slimb}-Ci^{155} encounter (Fig. 7d,e). This model explains the expression of CSN-dependent conditionally stable Ci^{155} in the low-to-intermediate Hh signalling regions, in which Ci^{155} may be released from the labile SCF^{Slimb}-Ci^{155} complex before SCF re-neddylation.

Substrate–SCF affinity is controlled by substrate phosphorylation and, in the case of Ci^{155}, the number of phospho groups on substrates. It was predicted that switch-like protein degradation could be achieved for substrates bearing multiple phosphorylation sites. For example, SCF-mediated Sic1 polyubiquitylation and degradation ensues at the G1–S transition when the number of phosphorylated sites on Sic1 reaches six, as Sic1 binding affinity to the F-box protein CDC4 increases dramatically from Sic1-5p to Sic1-6p[56]. Ci^{155} also bears multiple phosphorylation sites. Unlike Sic1, however, partial phosphorylation of Ci^{155} is meaningful in establishing low-to-intermediate responses to Hh signalling. The amount of Ci^{155} binding to Slimb increases incrementally with the number of phosphorylated sites[26], which precludes decisive proteolysis and allows the meta-stable SCF^{Slimb}-Ci^{155} intermediates for CSN regulation. In *CSN* mutant wing discs, responses to Hh signalling become more switch-like, as only low and high Hh signalling responses are detected. Thus, this study and previous studies[23–26,57] indicate that partial phosphorylation of Ci^{155} is essential, but not sufficient, for non-switch-like substrate proteolysis. CSN-mediated deneddylation has to be incorporated into the machinery for specific enhancement of Ci^{155} levels over a low threshold. Whether it is the enhanced levels of Ci^{155} or the reduced levels of the proteolysed Ci^{75} repressor that affect *dpp-lacZ* expression is unclear. This specific requirement of deneddylation in developing wings underscores the developmental role of CSN deneddylation at a tissue level. We also envision that CSN-mediated deneddylation of cullin-based ligases may modulate cellular levels of many other proteins in a context-dependent manner, thereby adjusting their biological readouts to meet distinct requirements of different cell contexts in a multicellular organism.

Methods

Fly genetics and fly stocks. *$Cul1^{EX12}$*, *$Nedd8^{AN01512}$*, *UAS-$CSN5^{42}$*, *UAS-$CSN5^{D148N42}$* and *UAS-flag-ago*[58]; *$CSN4^{null}$* and *$CSN5^{null59}$*; *UAS-HA-ci-3P*[22], *Tub-myc-slimb*, *UAS-myc-slimb-Δfbx*[47], *UAS-DN-GSK3β*[24], *UAS-DN-DBT*[25], *UAS-ci-myc*[26], *UAS-ci-C1-3E-myc*[26], *UAS-ci-G2-3E-myc*[26] and *$slimb^{P149313}$*; *UAS-PKA-R** and *UAS-PKA-mC** [60] have been described previously. BS3.0 *dpp-LacZ* and *ci-LacZ* were obtained from Bloomington stock center. *UAS-uba1-dsRNA* (stock ID: 1782R-2) was obtained from Fly Stocks of National Institute of Genetics. *hsflp*; *FRT42D ubi-nlsGFP*; *C765-GAL4/TM6B*, *ms1096-GAL4*, *hsflp*; *FRT42D ubi-nlsGFP*, *hsflp*; *ap-GAL4/CyO*; *FRT82B ubi-nlsGFP and ms1096-GAL4*, *hsflp*; *FRT82B ubi-nlsGFP* were used to generate *$CSN4^{null}$* and *$CSN5^{null}$* mutant clones that simultaneously express transgenes of interest. *ms1096-GAL4*, *hsflp*; *FRT82B tub-GAL80* was used to generate *$CSN5^{null}$* MARCM clones in wing pouches. *hsflp/+*, *FRT42D $Cul1^{EX}$*, *ubi-nlsGFP/FRT42D $CSN4^{null}$* was used to generate twin mutant clones for *$Cul1^{EX}$* and *$CSN4^{null}$*. *ms1096-GAL4*, *hsflp/+*; *FRT42D $Cul1^{EX}$*, *ubi-nlsGFP/FRT42D $CSN4^{null}$*; *UAS-DN-GSK3β/+* was used to generate twin mutant clones for *$Cul1^{EX}$* and *$CSN4^{null}$* in *DN-GSK3β*-expressing wing discs.

Flies were kept at 25 °C. At 48–72 h after egg laying, larvae were heat shocked at 37 °C for 1 h to generate *$CSN4^{null}$* and *$CSN5^{null}$* mutant clones. To generate *uba1-shRNA*-expressing *$CSN5^{null}$* MARCM clones, 72 h after egg laying, *ms1096-GAL4*, *hsflp/+*; *UAS-uba1-dsRNA/+*; *FRT82B $CSN5^{null}$/FRT82B tub-GAL80* larvae were heat shocked at 37 °C for 1 h.

Immunostaining and image processing. For immunostaining, dissected imaginal wing discs from wandering third-instar larvae were fixed in 4% formaldehyde in phosphate-buffered saline (PBS) solution for 17 min, washed with 0.3% triton X-100 in PBS (PBST) for 10 min (three times), blocked in PBST supplemented by 5% normal donkey serum for 30 min and incubated with primary antibodies of various dilutions in PBST containing 5% normal donkey serum for 16 h at 4 °C. These imaginal discs were washed with PBST for 10 min (three times), followed by a 2-h secondary antibody incubation before washes (three times in PBST). The stained wing discs were mounted on slides in PBS + 50% glycerol. All procedures were performed at 25 °C unless specifically described. The primary antibodies used were mouse anti-Flag (M2, 1:3,000; Sigma), mouse anti-Myc (9E10, 1:200; Santa Cruz Biotechnology), rat anti-full-length Ci (2A1, 1:10; Developmental Studies Hybridoma Bank), mouse anti-β-gal (1:1,000; Sigma) and mouse anti-Arm and mouse anti-En (1:100, N2-7A1 and 1:30, 4D9, respectively, Developmental Studies Hybridoma Bank). The secondary antibodies used were Cy3-conjugated goat anti-mouse IgG, Cy3-conjugated goat anti-rabbit IgG and Cy3-conjugated goat anti-rat IgG (1:1,000, Jackson ImmunoResearch Laboratories).

Images were acquired by Zeiss LSM510 META Confocal Imaging System (Zeiss). To quantify Ci^{155} expression levels in wild-type, *$CSN4^{null}$* and *$Cul1^{EX}$* cells, the maximal pixel intensities of Ci^{155} immunoreactivities in the A compartment were below 255 and set to be zero in the P compartment as background control by using Photoshop (Adobe).

References

1. Wolpert, L. Positional information and the spatial pattern of cellular differentiation. *J. Theor. Biol.* **25,** 1–47 (1969).
2. Osterfield, M., Kirschner, M. W. & Flanagan, J. G. Graded positional information: interpretation for both fate and guidance. *Cell* **113,** 425–428 (2003).
3. Ibanes, M. & Belmonte, J. C. Theoretical and experimental approaches to understand morphogen gradients. *Mol. Syst. Biol.* **4,** 176 (2008).
4. Jacob, L. & Lum, L. Hedgehog signaling pathway in Drosophila. *Sci. STKE* **2007,** cm7 (2007).
5. Ashe, H. L. & Briscoe, J. The interpretation of morphogen gradients. *Development* **133,** 385–394 (2006).
6. Wang, Y., McMahon, A. P. & Allen, B. L. Shifting paradigms in Hedgehog signaling. *Curr. Opin. Cell Biol.* **19,** 159–165 (2007).
7. Motoyama, J. Essential roles of Gli3 and sonic hedgehog in pattern formation and developmental anomalies caused by their dysfunction. *Congenit. Anom. (Kyoto)* **46,** 123–128 (2006).
8. Ruiz i Altaba, A., Mas, C. & Stecca, B. The Gli code: an information nexus regulating cell fate, stemness and cancer. *Trends Cell Biol.* **17,** 438–447 (2007).
9. Baker, N. E. Patterning signals and proliferation in Drosophila imaginal discs. *Curr. Opin. Genet. Dev.* **17,** 287–293 (2007).
10. Jiang, J. & Hui, C. C. Hedgehog signaling in development and cancer. *Dev. Cell* **15,** 801–812 (2008).
11. Aza-Blanc, P., Ramirez-Weber, F. A., Laget, M. P., Schwartz, C. & Kornberg, T. B. Proteolysis that is inhibited by hedgehog targets Cubitus interruptus protein to the nucleus and converts it to a repressor. *Cell* **89,** 1043–1053 (1997).
12. Ou, C. Y., Lin, Y. F., Chen, Y. J. & Chien, C. T. Distinct protein degradation mechanisms mediated by Cul1 and Cul3 controlling Ci stability in Drosophila eye development. *Genes Dev.* **16,** 2403–2414 (2002).
13. Jiang, J. & Struhl, G. Regulation of the Hedgehog and Wingless signalling pathways by the F-box/WD40-repeat protein Slimb. *Nature* **391,** 493–496 (1998).
14. Methot, N. & Basler, K. Suppressor of fused opposes hedgehog signal transduction by impeding nuclear accumulation of the activator form of Cubitus interruptus. *Development* **127,** 4001–4010 (2000).
15. Wang, Q. T. & Holmgren, R. A. Nuclear import of cubitus interruptus is regulated by hedgehog via a mechanism distinct from Ci stabilization and Ci activation. *Development* **127,** 3131–3139 (2000).
16. Wang, G., Amanai, K., Wang, B. & Jiang, J. Interactions with Costal2 and suppressor of fused regulate nuclear translocation and activity of cubitus interruptus. *Genes Dev.* **14,** 2893–2905 (2000).
17. Sisson, B. E., Ziegenhorn, S. L. & Holmgren, R. A. Regulation of Ci and Su(fu) nuclear import in Drosophila. *Dev. Biol.* **294,** 258–270 (2006).
18. Ingham, P. W. & McMahon, A. P. Hedgehog signaling in animal development: paradigms and principles. *Genes. Dev.* **15,** 3059–3087 (2001).
19. Hooper, J. E. & Scott, M. P. Communicating with Hedgehogs. *Nat. Rev. Mol. Cell Biol.* **6,** 306–317 (2005).
20. Jiang, J. Regulation of Hh/Gli signaling by dual ubiquitin pathways. *Cell Cycle* **5,** 2457–2463 (2006).
21. Price, M. A. & Kalderon, D. Proteolysis of cubitus interruptus in Drosophila requires phosphorylation by protein kinase A. *Development* **126,** 4331–4339 (1999).
22. Wang, G., Wang, B. & Jiang, J. Protein kinase A antagonizes Hedgehog signaling by regulating both the activator and repressor forms of Cubitus interruptus. *Genes Dev.* **13,** 2828–2837 (1999).
23. Price, M. A. & Kalderon, D. Proteolysis of the Hedgehog signaling effector Cubitus interruptus requires phosphorylation by Glycogen Synthase Kinase 3 and Casein Kinase 1. *Cell* **108,** 823–835 (2002).
24. Jia, J. *et al.* Shaggy/GSK3 antagonizes Hedgehog signalling by regulating Cubitus interruptus. *Nature* **416,** 548–552 (2002).
25. Jia, J. *et al.* Phosphorylation by double-time/CKIepsilon and CKIalpha targets cubitus interruptus for Slimb/beta-TRCP-mediated proteolytic processing. *Dev. Cell* **9,** 819–830 (2005).
26. Smelkinson, M. G. & Kalderon, D. Processing of the Drosophila hedgehog signaling effector Ci-155 to the repressor Ci-75 is mediated by direct binding to the SCF component Slimb. *Curr. Biol.* **16,** 110–116 (2006).
27. Chou, Y. H. & Chien, C. T. Scabrous controls ommatidial rotation in the Drosophila compound eye. *Dev. Cell* **3,** 839–850 (2002).

28. Lammer, D. *et al.* Modification of yeast Cdc53p by the ubiquitin-related protein rub1p affects function of the SCFCdc4 complex. *Genes Dev.* **12,** 914–926 (1998).
29. Hori, T. *et al.* Covalent modification of all members of human cullin family proteins by NEDD8. *Oncogene* **18,** 6829–6834 (1999).
30. Wu, J. T., Chan, Y. R. & Chien, C. T. Protection of cullin-RING E3 ligases by CSN-UBP12. *Trends Cell Biol.* **16,** 362–369 (2006).
31. Osaka, F. *et al.* Covalent modifier NEDD8 is essential for SCF ubiquitin-ligase in fission yeast. *EMBO J.* **19,** 3475–3484 (2000).
32. Lincoln, C., Britton, J. H. & Estelle, M. Growth and development of the axr1 mutants of Arabidopsis. *Plant Cell* **2,** 1071–1080 (1990).
33. del Pozo, J. C. *et al.* AXR1-ECR1-dependent conjugation of RUB1 to the Arabidopsis Cullin AtCUL1 is required for auxin response. *Plant Cell* **14,** 421–433 (2002).
34. Dharmasiri, S., Dharmasiri, N., Hellmann, H. & Estelle, M. The RUB/Nedd8 conjugation pathway is required for early development in Arabidopsis. *EMBO J.* **22,** 1762–1770 (2003).
35. Kawakami, T. *et al.* NEDD8 recruits E2-ubiquitin to SCF E3 ligase. *EMBO J.* **20,** 4003–4012 (2001).
36. Duda, D. M. *et al.* Structural insights into NEDD8 activation of cullin-RING ligases: conformational control of conjugation. *Cell* **134,** 995–1006 (2008).
37. Saha, A. & Deshaies, R. J. Multimodal activation of the ubiquitin ligase SCF by Nedd8 conjugation. *Mol. Cell* **32,** 21–31 (2008).
38. Pierce, N. W., Kleiger, G., Shan, S. O. & Deshaies, R. J. Detection of sequential polyubiquitylation on a millisecond timescale. *Nature* **462,** 615–619 (2009).
39. Lyapina, S. *et al.* Promotion of NEDD-CUL1 conjugate cleavage by COP9 signalosome. *Science* **292,** 1382–1385 (2001).
40. Schwechheimer, C. & Deng, X. W. COP9 signalosome revisited: a novel mediator of protein degradation. *Trends Cell Biol.* **11,** 420–426 (2001).
41. Bosu, D. R. & Kipreos, E. T. Cullin-RING ubiquitin ligases: global regulation and activation cycles. *Cell Div.* **3,** 7 (2008).
42. Wu, J. T., Lin, H. C., Hu, Y. C. & Chien, C. T. Neddylation and deneddylation regulate Cul1 and Cul3 protein accumulation. *Nat. Cell Biol.* **7,** 1014–1020 (2005).
43. Gusmaroli, G., Figueroa, P., Serino, G. & Deng, X. W. Role of the MPN subunits in COP9 signalosome assembly and activity, and their regulatory interaction with Arabidopsis Cullin3-based E3 ligases. *Plant Cell* **19,** 564–581 (2007).
44. He, Q., Cheng, P., He, Q. & Liu, Y. The COP9 signalosome regulates the Neurospora circadian clock by controlling the stability of the SCFFWD-1 complex. *Genes Dev.* **19,** 1518–1531 (2005).
45. Wee, S., Geyer, R. K., Toda, T. & Wolf, D. A. CSN facilitates Cullin-RING ubiquitin ligase function by counteracting autocatalytic adapter instability. *Nat. Cell Biol.* **7,** 387–391 (2005).
46. Cope, G. A. & Deshaies, R. J. Targeted silencing of Jab1/Csn5 in human cells downregulates SCF activity through reduction of F-box protein levels. *BMC Biochem.* **7,** 1 (2006).
47. Ko, H. W., Jiang, J. & Edery, I. Role for Slimb in the degradation of Drosophila Period protein phosphorylated by Doubletime. *Nature* **420,** 673–678 (2002).
48. Huang, X., Langelotz, C., Hetfeld-Pechoc, B. K., Schwenk, W. & Dubiel, W. The COP9 signalosome mediates beta-catenin degradation by deneddylation and blocks adenomatous polyposis coli destruction via USP15. *J. Mol. Biol.* **391,** 691–702 (2009).
49. Panattoni, M. *et al.* Targeted inactivation of the COP9 signalosome impairs multiple stages of T cell development. *J. Exp. Med.* **205,** 465–477 (2008).
50. Schweitzer, K., Bozko, P. M., Dubiel, W. & Naumann, M. CSN controls NF-kappaB by deubiquitinylation of IkappaBalpha. *EMBO J.* **26,** 1532–1541 (2007).
51. Zhang, Q. *et al.* A hedgehog-induced BTB protein modulates hedgehog signaling by degrading Ci/Gli transcription factor. *Dev. Cell* **10,** 719–729 (2006).
52. Blair, S. S. Engrailed expression in the anterior lineage compartment of the developing wing blade of Drosophila. *Development* **115,** 21–33 (1992).
53. Ou, C. Y., Wang, C. H., Jiang, J. & Chien, C. T. Suppression of Hedgehog signaling by Cul3 ligases in proliferation control of retinal precursors. *Dev. Biol.* **308,** 106–119 (2007).
54. Methot, N. & Basler, K. Hedgehog controls limb development by regulating the activities of distinct transcriptional activator and repressor forms of Cubitus interruptus. *Cell* **96,** 819–831 (1999).
55. Aikin, R. A., Ayers, K. L. & Therond, P. P. The role of kinases in the Hedgehog signalling pathway. *EMBO Rep.* **9,** 330–336 (2008).
56. Nash, P. *et al.* Multisite phosphorylation of a CDK inhibitor sets a threshold for the onset of DNA replication. *Nature* **414,** 514–521 (2001).
57. Smelkinson, M. G., Zhou, Q. & Kalderon, D. Regulation of Ci-SCFSlimb binding, Ci proteolysis, and hedgehog pathway activity by Ci phosphorylation. *Dev. Cell* **13,** 481–495 (2007).
58. Ho, M. S. *et al.* Gcm protein degradation suppresses proliferation of glial progenitors. *Proc. Natl Acad. Sci. USA* **106,** 6778–6783 (2009).
59. Oron, E. *et al.* COP9 signalosome subunits 4 and 5 regulate multiple pleiotropic pathways in Drosophila melanogaster. *Development* **129,** 4399–4409 (2002).
60. Li, W., Ohlmeyer, J. T., Lane, M. E. & Kalderon, D. Function of protein kinase A in hedgehog signal transduction and Drosophila imaginal disc development. *Cell* **80,** 553–562 (1995).

Acknowledgments

We thank H.H. Lee for detail discussion and editing the manuscript. We thank D. Kalderon, J. Jiang, Y.H. Liao, W.J. Wang and T.P. Yao for reagents and critical suggestions. We thank the staff of the Sixth Core Lab and DNA Sequencing Facility, Department of Medical Research, National Taiwan University Hospital for technical support. We also thank the Taiwan Fly Core Facility and Fly Core Facility in National Taiwan University for technical support. This work is supported by grant NSC 97-2320-B-002-054-MY3 from National Science Council, Taiwan and grant NHRI-EX99-9926SC from National Health Research Institutes, Taiwan to J.-T.W.

Author contributions

J.-T.W. designed and performed experiments, analysed data and wrote the paper. W.-H.L. helped design experiments for Figures 3 and 6 and wrote the paper. W.-Y.C. performed experiments for Supplementary Figure S3, Y.-C.H. performed experiments for Figure 4d, C.-Y.T. for microinjection, M.S.H. provided *UAS-flag-ago* transgene, H.P. designed and supervised experiments and analysed data for Figure 4d. C.-T.C. designed experiments, analysed data and wrote the paper.

Additional information

Supplementary Information accompanies this paper at http://www.nature.com/naturecommunications

Competing financial interests: The authors declare no competing financial interests.

Reprints and permission information is available online at http://npg.nature.com/reprintsandpermissions/

How to cite this article: Wu, J.-T. *et al.* CSN-mediated deneddylation differentially modulates Ci^{155} proteolysis to promote Hedgehog signalling responses. *Nat. Commun.* 2:182 doi: 10.1038/ncomms1185 (2011).